The Effect of Mn and Si on the Morphology and Kinetics of the Bainite Transformation in Fe-C-Ti Alloys

S.K. LIU and G.Y. ZHANG

The overall kinetics of the isothermal transformation of austenite to ferrite and bainite at intermediate temperatures and the microstructure of the transformation products in Fe-C-Ti, Fe-C-Ti-Si, Fe-C-Ti-Mn, and Fe-C-Ti-Mn-Si alloys were investigated with dilatometry, quantitative metallography, and TEM. The rate of transformation of austenite is retarded and the precipitation of carbide is inhibited in Ti-containing alloys by additions of Si, Mn, or Si + Mn. In addition to bainite and degenerate ferrite plates, a large amount of granular structure consisting of martensite and retained austenite (so-called granular bainite) is observed in these alloys if the isothermal reaction time is not long enough to complete austenite decomposition. It is suggested that the inhibiting effect of Si on carbide precipitation, the segregation of carbide-forming elements to prior γ grain boundaries and interphase interfaces, and the enhancing effect of Si on the segregation of these elements lead to the results obtained. The results also support the view that so-called granular bainite is a mixture of transformation products produced by the partial decomposition of austenite.

I. INTRODUCTION

INCREASING interest in the application of high-strength low-alloy steels (HSLA) has resulted in numerous investigations of the precipitation of TiC within these alloys and its effect on mechanical properties.[1,2] The formation of so-called granular bainite (GB), consisting of ferrite with a high dislocation density and austenite-martensite particles, during noncontrolled rolling of Ti-containing steels also has been studied;[2] however, there have been no investigations of the effect of Ti alone or combined with Si, Mn, and Mn + Si, respectively, on the transformation kinetics and the morphology of the transformation products. In addition, there is considerable confusion over the definition and classification of GB. The purpose of this paper is to investigate the effects of Ti concentration in Fe-C-Ti alloys and additions of Si, Mn, and Si + Mn on the microstructures formed at intermediate temperatures and the kinetics of the transformation. This investigation seeks to find out whether there is any fundamental difference between the precipitation of ferrite during bainite reaction and during the formation of the so-called GB structure. It is believed that these results will contribute to the understanding of the bainite transformation mechanism as a whole.

II. EXPERIMENTAL

Alloys used in this research were melted in a vacuum furnace from commercially pure iron, ferrotitanium, and

S.K. LIU, Professor, is with the Department of Materials Engineering, Southwest Jiaotong University, Chengdu Sichuan, 610031, People's Republic of China. G.Y. ZHANG, former Graduate Student, Southwest Jiaotong University, is Research Assistant, Institute of Locomotive and Vehicle Technology, Changzhou, Jiangsu, People's Republic of China.

high-purity (99.9 pct) silicon and manganese. The chemical compositions of the alloys are shown in Table I. Ingots were forged into bars with a cross section of 20 × 20 mm and homogenized at 1200 °C for 30 hours.

Cylindrical samples 3 mm in diameter and 10-mm long were heated to 1200 °C for 10 minutes in an autodilatometer (Formastor), and then quenched with a stream of He or N_2 to the reaction temperature. The initiation of transformation was determined by the inflection in the expansion vs time curve, but the fraction transformation was determined by the point-counting method.

Because alloys T1, T2, and T3 have short incubation times at intermediate temperatures, the quenching ability of He is insufficient to ensure isothermal transformation; hence, some samples were austenitized in a salt bath and isothermally transformed in a lead pot. Transmission Electron Microscopy (TEM) observations were carried out with a H-700H microscope using a 200 kV accelerating voltage. Specimens were final-polished with a double-jet polisher in 10 pct perchloric acid–90 pct ethanol solution at approximately −30 °C and a potential of 50 V.

III. RESULTS

A. Fe-C-Ti Alloy

The TTT curves of alloys T1, T2, and T3 are shown in Figure 1. It can be seen that the rate of decomposition of austenite decreases with increases in Ti content. The optical micrographs in Figure 2 show the microstructures of alloy T1 isothermally treated at 550 °C for different times. From Figure 2(a), it can be seen that the bainite reaction is approximately completed after 3 seconds. The microstructure is characteristic of upper bainite. Ferrite plates which have nearly the same orientation constitute a packet. The granular structure can be observed in some regions (see arrows). After 20 seconds (Figure 2(b)), the plates partially coalesce so that some of the packets develop a massive or blocky contour. The original ferrite plates can no longer be distinguished; only faint traces of the original plates can be

**Table I. Chemical Composition
of the Alloys (Weight Percent)**

Alloys	C	Ti	Si	Mn
T1	0.155	0.11	—	—
T2	0.116	0.17	—	—
T3	0.150	0.32	—	—
TS	0.140	0.11	0.62	—
TM	0.140	0.10	—	1.96
TSM	0.148	0.10	0.40	2.03

seen within the packets. This phenomenon becomes more obvious as the reaction time increases (Figure 2(c)).

Transmission electron microscopy micrographs of alloy T1 transformed at 550 °C for 20 seconds are shown in Figure 3. The lath structure can still be observed within a packet which looks like a blocky ferrite under the optical microscope. Figures 3(b) and (c) show interlath and intralath carbide precipitation. In some regions, interlath islands and films of austenite, which were isolated by growing ferrite plates, turn to martensite during quenching (Figure 3(d)). Some of the austenite islands between ferrite laths decompose to degenerate pearlite (Figure 4(a)) at longer reaction times. Carbides can also be seen at packet boundaries and prior γ grain boundaries (Figure 4(b)). All of the carbides mentioned above were identified with selected area diffraction (SADP) as cementite. Precipitation of TiC on dislocation within ferrite was observed in specimens reacted longer than approximately 600 seconds. The dislocation density of ferrite also decreased with increased reaction time.
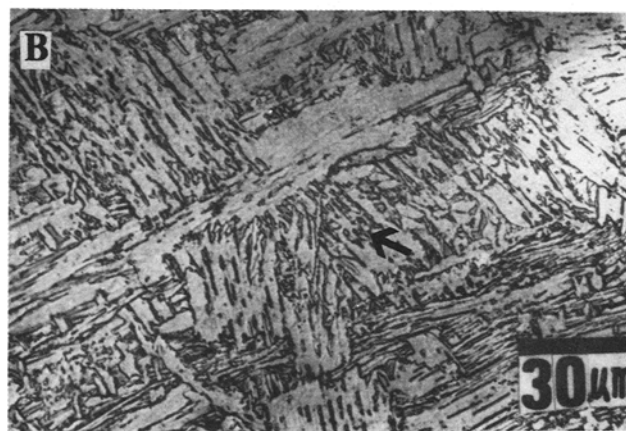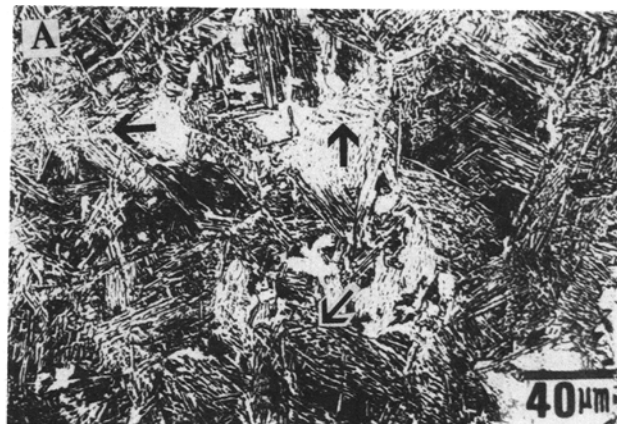

Fig. 2—Microstructure of alloy T1 transformed at 550 °C for (a) 3 sec (granular bainite regions are shown with arrows), (b) 20 sec (part of the ferrite plates have coalesced so that some of the bainite packets develop a massive contour), and (c) 300 sec (most of the original bainite packets develop a massive contour).
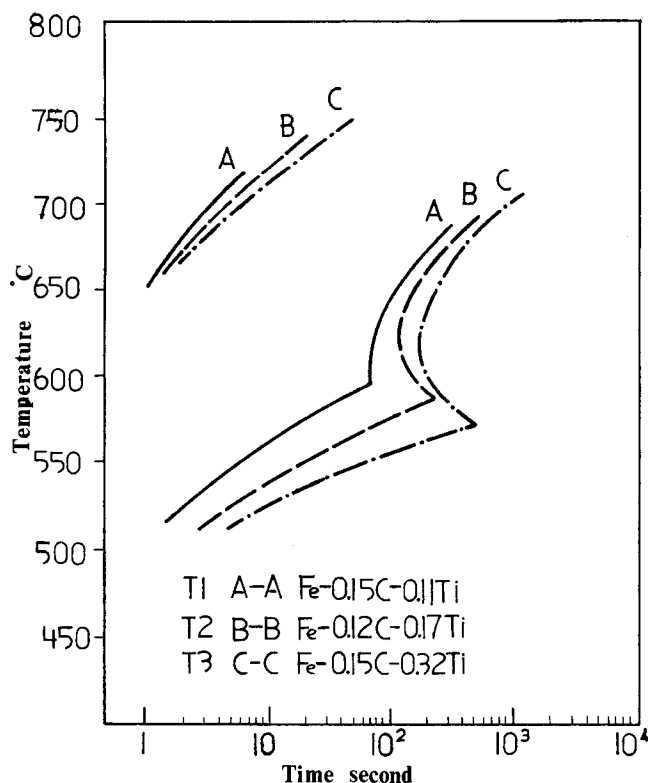

Fig. 1—Initial (1 pct) and finish curves of TTT diagram of alloys T1, T2, and T3.

B. *Fe-C-Ti-Mn, Fe-C-Ti-Si, and Fe-C-Ti-Mn-Si Alloys*

The TTT curves for Fe-0.14C-0.1Ti alloys containing Mn, Si, or Mn and Si together are shown in Figure 5. These alloys have a slower rate of austenite decomposition compared with the Fe-C-Ti alloys in Figure 1. This
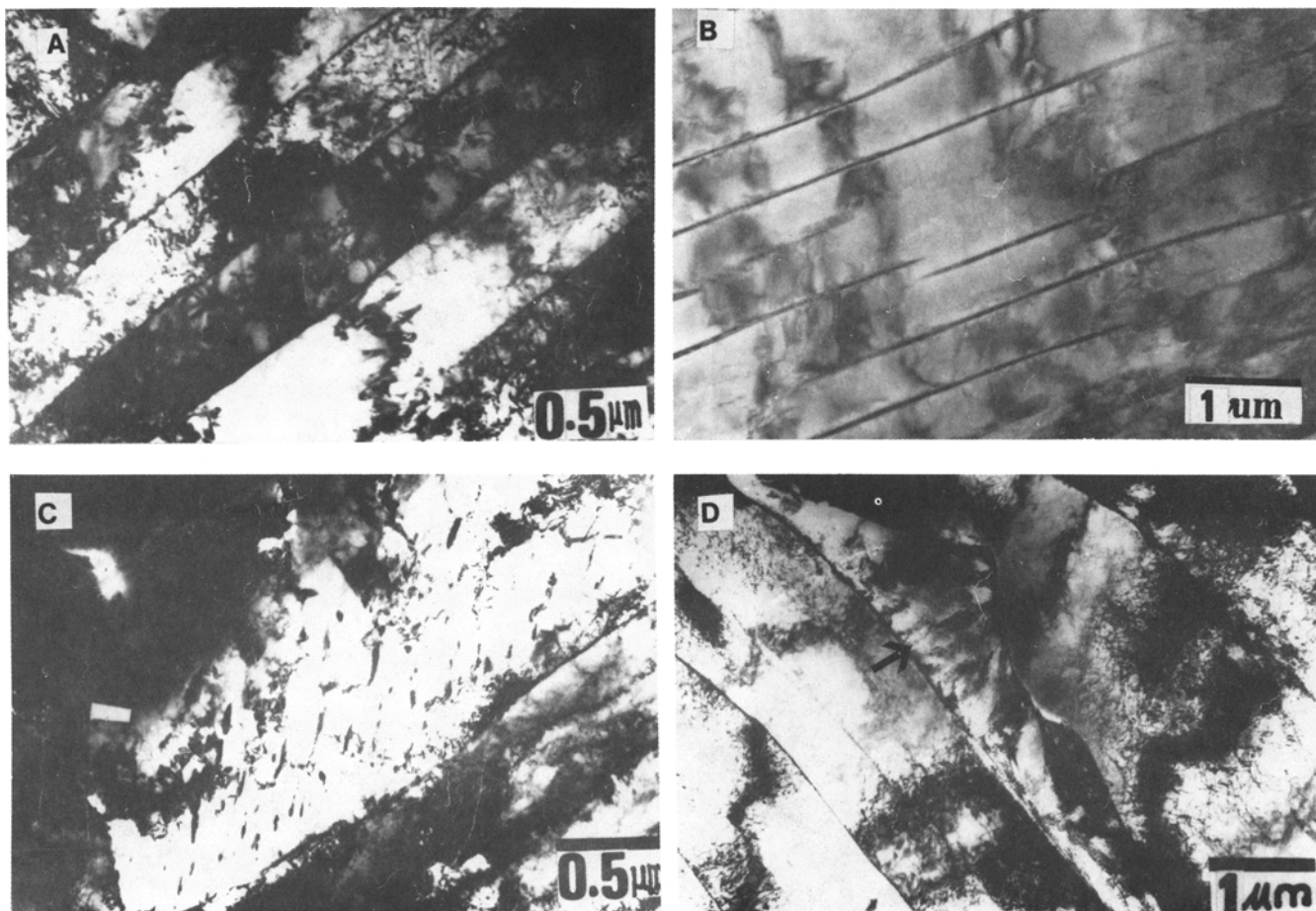
Fig. 3—TEM micrographs of alloy T1 transformed at 550 °C for 20 sec: (a) ferrite lath, (b) interlath carbide, (c) intralath carbide, and (d) (M + A) structure (see arrow) and ferrite lath.

means that any of the Ti-Si, Ti-Mn, and Ti-Mn-Si combinations makes austenite more stable. Not only is the incubation time longer, but the interval between the start and finish of transformation is increased.

Figure 6(a) shows an optical micrograph of alloy TM after isothermal transformation for 900 seconds at 550 °C. The intragranular ferrite appears more degenerate with fewer well-formed plates relative to the ferrite morphology in the Mn-free alloy shown in Figure 2. Figure 6(b) shows the microstructure of the same alloy isothermally treated for 3600 seconds at 500 °C. It consists of ferrite plates of various orientations and the granular martensite-austenite structure (M + A). Alloy TS has similar microstructural characteristics (Figure 6(c)), but most of the ferrite plates are parallel and nucleate at prior γ grain boundaries.

From the TEM image shown in Figure 7, it can be seen that numerous martensite and austenite islands (M + A) are present in addition to bainite and degenerate pearlite. Thus, it is evident that the granular structures shown in Figure 6 are what Habraken[1] has termed "granular bainite." The TS and TSM alloys have the same microstructural characteristics as the TM alloy, but alloy TSM has a greater tendency to form (M + A) islands.

The TM and TSM alloys have a stronger tendency to develop degenerate ferrite plates within the γ grains rather than at the prior γ grain boundaries; hence, most of the (M + A) islands isolated by the degenerate ferrite plates have a blocky shape. It has been demonstrated that the broad face of bainitic ferrite has a semicoherent interface with austenite;[3,4] thus, it appears facetted even in TEM micrographs (Figure 7). In the case of blocky (M + A) islands, not only the broad face of ferrite but also the growing tip of the ferrite plates have a flat interface; therefore, huge ledges appear on the ferrite/martensite interfaces.

C. Completeness of the Bainite Transformation

The interlath austenite films and the blocky austenite islands which form in the alloys of this investigation can decompose completely into various morphologies of $\alpha + Fe_3C$, including bainite, within a period of approximately 1000 seconds at 550 °C to 500 °C. The dilatation which accompanies this decomposition is quite small, and care must be exercised to detect the dilatation changes, ΔL, with time. The higher the Ti content of the alloy, the longer the time required to complete the transformation.

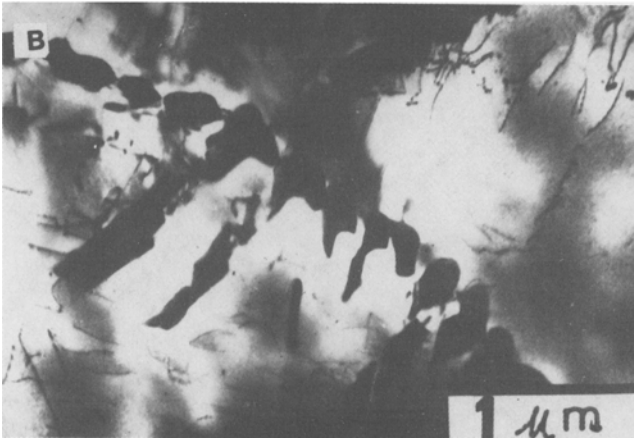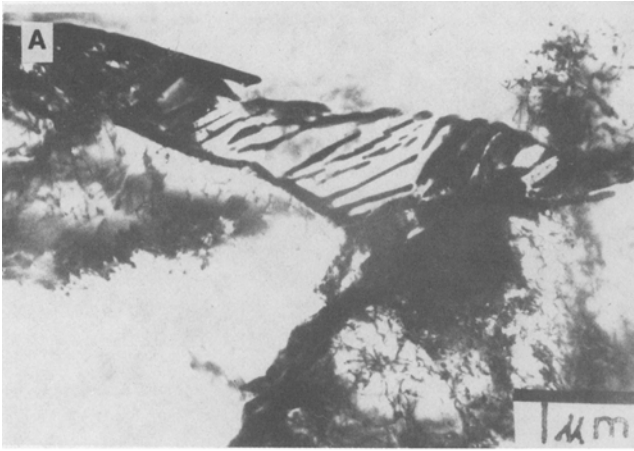The presence of Si, Mn, or Si + Mn in the TS, TM,

Fig. 4—TEM micrographs of alloy T1 transformed at 550 °C for 10 min: (a) degenerate pearlite and ferrite and (b) carbide precipitated at boundary (dislocations can be seen within the ferrite).

Fig. 5—Initial (1 pct) and finish curves of TTT diagram of alloys TS, TM, and TSM.

TS A-A Fe-0.14C-0.11Ti-0.62Si
TM B-B Fe-0.14C-0.10Ti-1.96Mn
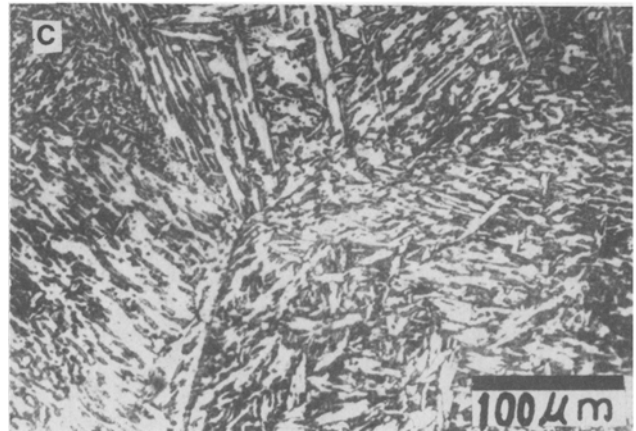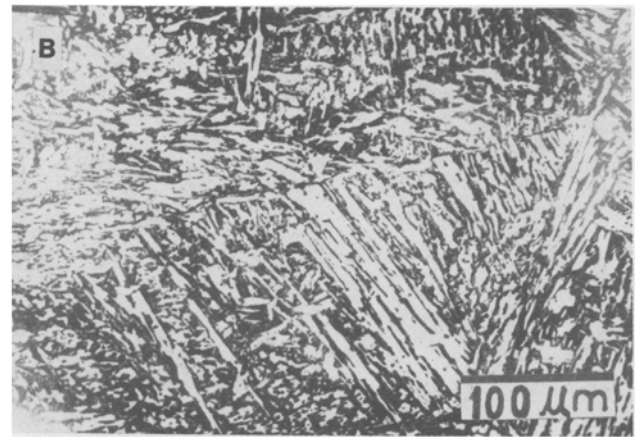TSM C-C Fe-0.15C-0.10Ti-0.40Si-2.03Mn

Fig. 6—Microstructures of alloys TM and TS: (a) TM alloy transformed at 550 °C for 900 sec, degenerate ferrite plates (white areas) and (M + A) islands, (b) TM alloy transformed at 500 °C for 3600 sec (the same as (a)), and (c) TS alloy transformed at 550 °C for 300 sec (the same as (a)).

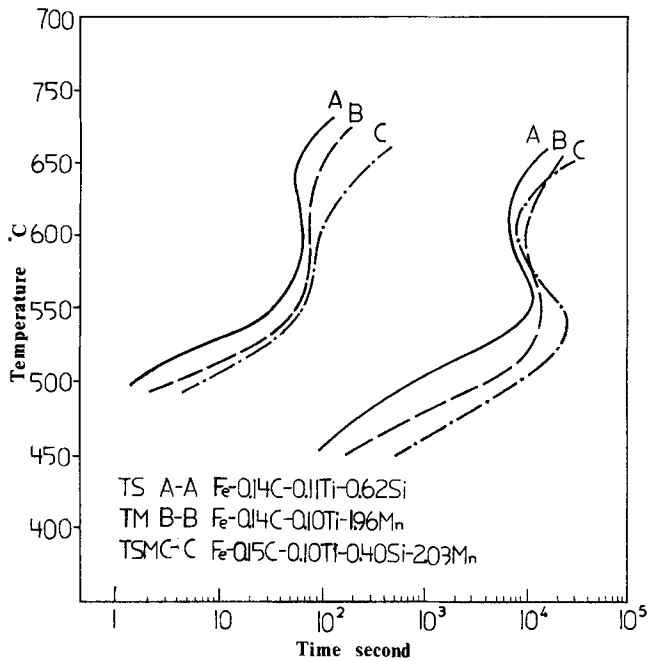or TSM alloys greatly increases the time required for completion of the decomposition of austenite. Most of the (M + A) islands remain unchanged for isothermal reaction times up to 10^4 seconds, the longest time employed in this study (see Figure 7).
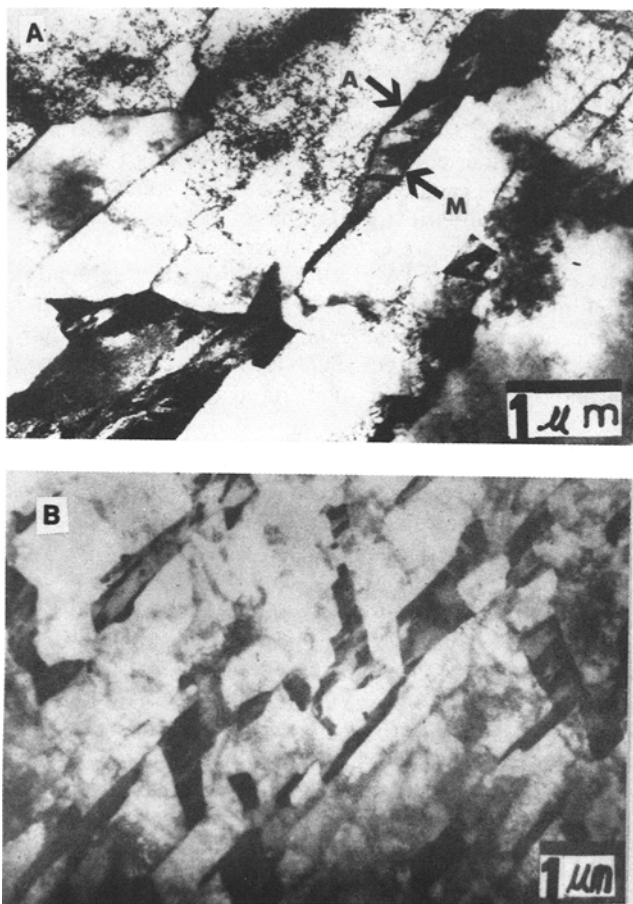
Fig. 7—TEM micrograph of alloys TM and TSM: (a) the (M + A) structure (shown with arrows M and A) in TM alloy transformed at 500 °C for 900 sec and (b) the (M + A) structure in TSM alloy transformed at 500 °C for 2.5 h.

IV. DISCUSSION

A. Kinetics

Titanium is one of the strong carbide-forming elements, and it decreases the activity of carbon in austenite (a_γ^c).[5] Hence, it is a candidate for producing a solute drag-like effect (SDLE)[3] by segregating to α/γ interfaces and retarding carbon diffusion away from these interfaces. The degregation of Ti to prior γ grain boundaries gives rise to a suppression of ferrite nucleation. As a result, the overall kinetics of $\gamma \rightarrow \alpha$ transformation decrease. The fact that Ti shifts the TTT curve only a small amount for the start of transformation may be attributed to the small amount of Ti present in these alloys and to the small solubility of Ti in austenite. Much of the Ti in the alloy becomes incorporated into the carbides and is, thus, unavailable to produce an SDLE.

Figure 1 also shows that the bay in the TTT curve becomes deeper with increasing Ti content. This is consistent with the SDLE concept;[6] i.e., the greater the Ti content, the more it segregates and the stronger the SDLE is. In addition, the location of the bay shifts to lower temperatures as the Ti content increases. According to the analysis of Banerji and Morral,[7] the depression of

the nose of the TTT curve might mean that most of the effective nucleating sites at prior austenite grain boundaries are occupied by segregated species, and greater undercooling is required to activate less favorable nucleation sites for ferrite. Adding Si, Mn, or Si + Mn to Fe-C-Ti alloys greatly reduces $\gamma \rightarrow \alpha$ transformation kinetics, making the TTT curves shift to longer times.

With respect to the role of Mn in the kinetics of transformation, it is considered that on the basis of a relation given by Guttmann and McLean[8] to describe equilibrium segregation and the positive interaction coefficient between C and Mn, α', the presence of Mn will promote the cosegregation of C and Mn at grain boundaries. From one of the authors' investigations, it is established that Mn also segregates to prior γ boundaries by a nonequilibrium segregation process.[9] Furthermore, Mn decreases the activity of carbon in austenite[5] and, thus, hinders the bainite transformation when added to Fe-C-Ti alloys through an SDLE.

Although Si increases value a_γ^c, it still exerts a hindering effect on the decomposition of austenite due to the inhibiting effect of Si on carbide precipitation. It is evident that the absence of carbide precipitation accompanying ferrite formation leads to carbon enrichment of austenite adjacent to ferrite plates. The higher carbon concentration in this austenite lowers the driving force for subsequent precipitation of ferrite.[10] In addition, from the result given by McMahon,[11] Si has a weak interaction with C; i.e., the interaction coefficient of Si and C, α', is negative. According to Guttmann's analysis, the relative repulsion between Si and C yields $\alpha' < 0$, segregation of C repels Si from both γ grain boundaries, and α/γ interfaces, in turn, increase the driving force for further C segregation. The positive α' between C and Ti increases the segregation of both solutes; as a result, Si in Fe-C-Ti or Fe-C-Ti-Si-Mn alloys promotes the segregation of Ti and C. In particular, due to its suppression of carbide precipitation, the addition of Si in the alloy has an effect on transformation kinetics similar to that of increasing Ti. The same is true when Si and Mn are added together to an Fe-C-Ti alloy. Silicon promotes the segregation of Mn and Ti; thus, the TSM alloy has the slowest rate of transformation, as shown in Figure 1.

B. Microstructure

Interphase boundary precipitation of TiC is common in Ti-containing steels isothermally transformed at temperatures above 600 °C, but it is rare at reaction temperatures below 600 °C.[12] This is also the case in our investigation. In addition, even though TiC is thermodynamically more stable than cementite,[13] cementite precipitation is kinetically favored at low temperatures, presumably because of the requirement of long-range diffusion of Ti during TiC formation.

The precipitation of carbides in Fe-C-V, Fe-C-Ti, and Fe-C-Ni alloys has been previously reported.[13] It has been shown that VC precipitation on dislocations occurs even in an Fe-0.27V-0.05C alloy isothermally transformed at 740 °C for 2.5 hours. Evidently, the supersaturation of C and V and the subsequent precipitation of VC on dislocations are not limited to products of a

shear transformation. Thus, the C supersaturation inferred from TiC precipitation on dislocations in bainitic ferrite does not confirm that bainite forms by a shear mechanism. It is likely that Ti segregates to dislocations to reduce the strain energy induced by the size misfit between Fe and Ti atoms. Moreover, as mentioned above, Ti has a lower mobility. Thus, TiC precipitation on dislocations is reasonable since bainitic ferrite contains a high dislocation density. The orientation relationship between TiC and the matrix is also different from that in tempered martensite and lower bainite. At least three variants of the Baker-Nutting relationship are observed in the case of dislocation precipitation.[14]

In alloys T1, T2, and T3, the morphology of Fe_3C is altered, TiC precipitated on dislocations, and a lower fraction of (M + A) islands are observed. As mentioned before, segregation of Ti and Mn to prior γ grain boundaries and to α/γ interphase interfaces is suggested to increase with the addition of Si and Mn to the base alloy. Hence, in the TM, TS, and TSM alloys, it is unusual to observe carbides in samples reacted for a short time; thus, the carbon concentration of the untransformed austenite is raised considerably. This causes austenite to transform to a (M + A) structure after quenching. If the sample is isothermally transformed at 500 °C to 600 °C for longer times, regardless of whether it is the TM, TS, or TSM alloys, the untransformed austenite is expected to decompose into an aggregate of α + carbide. In the Fe-C-Ti alloys, 1200 seconds is sufficient for the complete decomposition of the blocky austenite and the interlath films of austenite. However, for the TM, TS, and TSM alloys, longer times are required for the blocky regions of austenite to decompose completely. Because the longest holding time employed in this investigation was only 10^4 seconds, only parts of the blocky austenite were decomposed in the latter alloys. From the results mentioned here, it is recognized that the so-called granular bainite structure is actually the product of the partial decomposition of austenite to bainite and ferrite. There is no basic difference between the ferrite constituent of so-called GB and that of classical bainite.
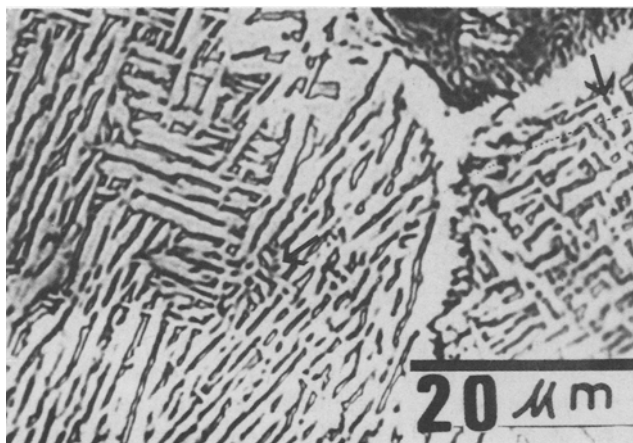

Fig. 8 — Microstructure of the Fe-0.38C-1.73Si alloy transformed at 450 °C for 20 sec. It consists of ferrite lath and retained austenite (some of the retained austenite regions have a granular morphology (see arrow)).

Figure 8 shows the microstructure of an Fe-0.38C-2.13Si alloy isothermally transformed at 450 °C for 20 seconds. It consists of lath ferrite and interlath retained austenite due to the inhibiting effect of Si on the formation of carbides. Since Si does not segregate to prior γ grain boundaries, these boundaries remain effective nucleation sites, and most of the ferrite plates initiate from these boundaries. This situation allows most of the ferrite plates in the Fe-C-Si alloy to grow parallel to each other. In the TSM, TM, and TS alloys, the segregation of Ti and Mn to the interfaces of growing ledges which are incoherent inhibits the lengthwise growth of the ledges; hence, ferrite plates become shorter and even have blocky morphology due to their more rapid thickening.

V. SUMMARY

1. Titanium increases the hardenability of Fe-C alloys and promotes the appearance of a bay in the TTT curve. Adding Si, Mn, or Mn + Si to a base Fe-C-Ti alloy also increases the hardenability to a greater extent. Segregation of Ti and Mn to α/γ interfaces and the enhancement of segregation of these elements by the interaction of Ti and Mn with Si might lead to these results.
2. In Fe-C-Ti alloys, the interlath films of austenite and the small amount of blocky austenite regions readily decompose into an aggregate of α and carbide. In TM, TS, and TSM alloys, carbide is not easily precipitated within the austenite, and carbon-enriched austenite transforms to martensite and retained austenite upon quenching. This is the typical microstructure of so-called granular bainite. In fact, GB may be considered as a structure resulting from the interrupted transformation of austenite to bainite and ferrite. There is no fundamental difference with respect to the formation mechanism or the substructure of the ferrite constituent between bainite and the GB structure. The mixture of ferrite, martensite, and retained austenite referred to as GB should be called the granular structure, since it is not really bainite under the microstructural definition of bainite.
3. The TiC precipitates on dislocations within ferrite in Fe-C-Ti alloys isothermally treated at temperatures below 600 °C for more than 600 seconds. This observation does not provide any evidence that this kind of ferrite is formed by a shear mode. The reduction of strain energy and the lower mobility of Ti might promote the precipitation of TiC on dislocations.

ACKNOWLEDGMENTS

REFERENCES

1. L.J. Habraken: *4th Int. Conf. on Electron Microscopy*, 1960, p. 621.

2. X. Cheng and M.G. Akben: in *HSLA Steel '85*, J.M. Gray, T. Ko, S.H. Zhang, B.R. Wu, and X.S. Xie, eds., ASM, Metals Park, OH, 1985, pp. 121-33.
3. J.M. Rigsbee and H.I. Aaronson: *Acta Metall.*, 1979, vol. 27, pp. 365-76.
4. C. Li, V. Perovic, and G.R. Purdy: in *Phase Transformation '87*, G.W. Lorimer, ed., Institute of Metals, London, 1988, pp. 326-29.
5. B. Uhrenius: *Scand. J. Metall.*, 1977, vol. 6, pp. 83-89.
6. H.I. Aaronson, S.K. Liu, W.T. Reynolds, Jr., G.J. Shiflet: *J. Mater. Sci.*, 1985, vol. 20, pp. 4232-38.
7. S.K. Banerji and J.E. Morral: *Boron in Steel*, TMS-AIME, Warrendale, PA, 1979.
8. M. Guttmann and D. McLean: *Interfacial Segregation*, ASM, Metals Park, OH, 1979, pp. 251-348.
9. S.K. Liu and J. Zhang: *Metall. Trans. A*, 1990, vol. 21A, pp. 1517-25.
10. W.T. Reynolds, Jr., S.K. Liu, F.Z. Li, S. Hartfield, and H.I. Aaronson: *Metall. Trans. A*, 1990, vol. 21A, pp. 1479-91.
11. C.J. McMahon: *Metall. Trans. A*, 1980, vol. 11A, pp. 531-35.
12. R.W.K. Honeycombe and F.B. Pickering: *Metall. Trans.*, 1972, vol. 3, pp. 1099-112.
13. R.W.K. Honeycombe: *Steels Microstructure and Properties*, Edward Arnod, London, 1981, p. 60.
14. R.W.K. Honeycombe: *Phase Transformations in Ferrous Alloys*, TMS-AIME, Warrendale, PA, 1984, pp. 259-80.